RESEARCH ARTICLE

Prominent White Matter Involvement in Multiple System Atrophy of Cerebellar Type

Jennifer Faber, MD,[1,2*] Ilaria Giordano, MD,[1,2] Xueyan Jiang, MS,[1] Christine Kindler, MD,[1,2] Annika Spottke, MD,[1,2] Julio Acosta-Cabronero, PhD,[3] Peter J. Nestor, MD, PhD,[4,5] Judith Machts, PhD,[6,7] Emrah Düzel, MD, PhD,[6,7] Stefan Vielhaber, MD,[6,7] Oliver Speck, PhD,[6,8,9] Ales Dudesek, MD,[10] Christoph Kamm, MD,[10] Lukas Scheef, MD, PhD,[1,11] and Thomas Klockgether, MD, PhD[1,2]

[1]*Clinical Research, German Center for Neurodegenerative Diseases, Bonn, Germany*
[2]*Department of Neurology, University Hospital Bonn, Germany*
[3]*Tenoke Ltd., Cambridge, United Kingdom*
[4]*Queensland Brain Institute, University of Queensland, Brisbane, Australia*
[5]*Neuroscience and Cognitive Health Program, Mater Hospital, South Brisbane, Australia*
[6]*German Center for Neurodegenerative Diseases, Magdeburg, Germany*
[7]*Department of Neurology, Otto-von-Guericke University, Magdeburg, Germany*
[8]*Department of Biomedical Magnetic Resonance, Faculty for Natural Sciences, Otto-von-Guericke University, Magdeburg, Germany*
[9]*Center for Behavioral Brain Sciences, Magdeburg, Germany*
[10]*Department of Neurology, University of Rostock, Rostock, Germany*
[11]*Department of Radiology, University of Bonn, Bonn, Germany*

ABSTRACT: Background: Sporadic degenerative ataxia patients fall into 2 major groups: multiple system atrophy with predominant cerebellar ataxia (MSA-C) and sporadic adult-onset ataxia (SAOA). Both groups have cerebellar volume loss, but little is known about the differential involvement of gray and white matter in MSA-C when compared with SAOA.
Objectives: The objective of this study was to identify structural differences of brain gray and white matter between both patient groups.
Methods: We used magnetic resonance imaging to acquire T1-weighted images and diffusion tensor images from 12 MSA-C patients, 31 SAOA patients, and 55 healthy controls. Magnetic resonance imaging data were analyzed with voxel-based-morphometry, tract-based spatial statistics, and tractography-based regional diffusion tensor images analysis.
Results: Whole-brain and cerebellar-focused voxel-based-morphometry analysis showed gray matter volume loss in both patient groups when compared with healthy controls, specifically in the cerebellar areas subserving sensorimotor functions. When compared with controls, the SAOA and MSA-C patients showed white matter loss in the cerebellum, whereas brainstem white matter was reduced only in the MSA-C patients. The tract-based spatial statistics revealed reduced fractional anisotropy within the pons and cerebellum in the MSA-C patients both in comparison with the SAOA patients and healthy controls. In addition, tractography-based regional analysis showed reduced fractional anisotropy along the corticospinal tracts in MSA-C, but not SAOA.
Conclusion: Although in our cohort extent and distribution of gray and white matter loss were similar between the MSA-C and SAOA patients, magnetic resonance imaging data showed prominent microstructural white matter involvement in the MSA-C patients that was not present in the SAOA patients. Our findings highlight the significance of microstructural white matter changes in the differentiation between both conditions. © 2020 The Authors. *Movement Disorders* published by Wiley Periodicals, Inc. on behalf of International Parkinson and Movement Disorder Society.

Key Words: diffusion tensor imaging; multiple system atrophy; sporadic ataxia; voxel based morphometry

***Correspondence to:** Dr. Jennifer Faber, Deutsches Zentrum für Neurodegenerative Erkrankungen, Klinische Forschung, Venusberg-Campus 1, 53127 Bonn, Germany; E-mail: jennifer.faber@dzne.de

Relevant conflicts of interests/financial disclosures: Nothing to report.

Received: 4 August 2019; **Revised:** 27 December 2019; **Accepted:** 30 December 2019

Published online 29 January 2020 in Wiley Online Library (wileyonlinelibrary.com). DOI: 10.1002/mds.27987

Progressive ataxia frequently starts in adults without a familial background. These patients may suffer from an acquired ataxia, such as alcoholic cerebellar degeneration or paraneoplastic cerebellar degeneration. Others have a genetic cause despite negative family history.[1-3] In the majority of these patients, however, a genetic or acquired cause of ataxia cannot be identified suggesting a sporadic degenerative ataxia.

Sporadic degenerative ataxia patients fall into 2 major groups. In 1 group, the underlying brain disease is multiple system atrophy (MSA). MSA is characterized by widespread degeneration of the cerebellum, brainstem, basal ganglia, and spinal cord. Some of these patients have prominent degeneration of cerebellum and brainstem and typically present with sporadic ataxia (MSA with predominant cerebellar ataxia [MSA-C]), whereas those with prominent basal ganglia degeneration suffer from parkinsonism (MSA with predominant parkinsonism). The definitive diagnosis of MSA requires demonstration of oligodendroglial inclusions at autopsy,[4,5] but a probable diagnosis can be made with high predictive accuracy on clinical grounds alone. The essential diagnostic feature of MSA is severe autonomic failure defined by orthostatic blood pressure drop of at least 30 mmHg systolic after standing from a recumbent position or urinary incontinence.[6] The second group of sporadic ataxia is clinically distinguished from MSA-C by the lasting absence of severe autonomic failure. These patients have been designated as idiopathic late-onset cerebellar ataxia or sporadic adult onset ataxia (SAOA) of unknown etiology.[7,8] The few SAOA cases that have come to autopsy had degeneration restricted to the cerebellar cortex and inferior olives,[9,10] but it is not clear whether SAOA is a disease entity or rather a group of different conditions presenting with a uniform clinical syndrome of progressive cerebellar ataxia. Compared with MSA, SAOA takes a more benign course.[11,12] In the first years after ataxia onset, a distinction between MSA-C and SAOA is often not possible, as severe autonomic failure defining MSA-C may only manifest several years after ataxia onset.

Atrophy of the cerebellum and brainstem are common features of MSA-C and SAOA.[13-22] In addition, microstructural alterations of the white matter have been reported in previous studies in MSA-C patients.[21-24] We used multimodal imaging approach to assess structural alteration of the brain in a deeply phenotyped cohort of MSA-C and SAOA patients to identify magnetic resonance imaging (MRI) parameters that might help to differentiate both conditions.

Methods

Participants

All patients were participants of the SPORTAX study, a prospective natural history study that longitudinally assessed the disease course of sporadic ataxia in elderly patients sporadic degenerative ataxia with adult onset: natural history study (SPORTAX-NHS).[11] The SPORTAX inclusion criteria are as follows: (1) progressive ataxia, (2) ataxia onset after the age of 40 years, (3) informative and negative family history (no similar disorders in first-degree and second-degree relatives; parents older than 50 years, or, if not alive, age at death of more than 50 years; no consanguinity of parents), and (4) no established acquired cause of ataxia (for details see Supporting Information Table 1). Participants were classified as MSA-C if they fulfilled the criteria for clinically probable MSA-C as defined in the second consensus statement by Gilman and colleagues.[6] In particular, all MSA-C patients presented with autonomic failure (Supporting Information Table 1 and Supporting Information Table 3). Participants not fulfilling the criteria for clinically probable MSA-C were classified as SAOA. The SPORTAX assessment protocol includes the Unified Multiple System Atrophy Rating Scale,[25] the Scale for the Assessment and Rating of Ataxia (SARA),[26] and the Inventory of Non-Ataxia Signs (INAS).[27] Detailed group characteristics are given in Table 1 and Supporting Information Table 3.

At 2 SPORTAX study sites (Bonn and Magdeburg), a MRI was acquired on all participants who gave consent and were able and willing to undergo MRI. To compare patient groups with healthy controls, we used MRI scans of healthy controls who participated in parallel studies using the identical MRI protocol. MRI scans of 12 MSA-C patients, 31 SAOA patients, and 55 healthy controls were included in the analysis (for details, see Supporting Information Table 2).

The study was approved by the local ethics committees. All participants provided written informed consent. This study is registered with ClinicalTrials.gov (NCT02701036).

TABLE 1. Demographic characteristics of the study population

Group	Number (Site BN/Site MD)	Mean Age at Scan (Min–Max, SD)	Male (Percentage)	Mean Age of Onset (SD)	Mean Disease Duration in Years (SD)	Mean SARA Sum Score (SD)	Mean INAS Score (SD)	Mean UMSARS II Score (SD)
SAOA	31 (6/25)	64.2 (43–80, 10.6)	18 (58.1)	57.1 (10.6)	7.1 (5.5)[a]	13.2 (1.4)[a]	1.68 (1.3)[a]	13.2 (6.1)[a]
MSA-C	12 (9/3)	62.8 (46–74, 7.7)	7 (58.3)	58.5 (7.3)	4.0 (1.7)[a]	17.0 (3.7)[a]	4.33 (1.6)[a]	22.5 (8.2)[a]
HC	55 (18/37)	64.7 (46–78, 8.0)	21 (38.2)	NA	NA	NA	NA	NA

BN, Bonn; MD, Magdeburg; Min = minimum; Max = maximum; SD, standard deviation; SARA, Scale for the Assessment and Rating of Ataxia; INAS, Inventory of Non-Ataxia Signs; UMSARS, Unified Multiple System Atrophy Rating Scale; SAOA, sporadic adult-onset ataxia; MSA-C, multiple system atrophy with predominant cerebellar ataxia; HC, healthy control; NA, not available.
[a]Significant difference between SAOA and MSA-C patients, $P < 0.01$.

Imaging Acquisition and Preprocessing

MRIs were acquired at both sites using a Siemens 3T scanner (Trio Tim in Bonn and Verio in Magdeburg, both Siemens Medical Systems, Erlangen, Germany). Both sites were equipped with the same gradient system and head coils (32 channel head coil) and used the same software release and MRI protocols.

Isotropic structural T1 images were acquired using a magnetization-prepared rapid gradient echo sequence with the following parameters: repetition time (TR) = 2500 ms, echo time (TE) = 4.37 ms, inversion time (TI) = 1100 ms, flip angle = 7°, receiver bandwith 140 Hz/Px, field of view = 256 mm × 256 mm × 192 mm with a voxel size of 1 mm isotropic, partial Fourier factor 7/8, and parallel imaging acceleration factor 2 (24 integrated reference lines) along the primary phase endcoding direction (anterior – posterior). Diffusion-weighted images were acquired using a twice-refocused single-shot echo planar imaging sequence with the following parameters: TR = 12100 ms, TE = 88 ms, field of view = 240 mm x 240 mm, 72 axial slices, with a voxel size of 2 mm isotropic, 1 scan without diffusion weighting (b0), and 30 diffusion-encoding directions with a b-value of 1000s/mm^2.

To reduce the sources of variance between scanners, several steps were taken before starting the study to harmonize the imaging methods across the participating sites. Both sites used SIEMENS scanners, and the imaging sequences were identical. The scans were acquired following the guidelines of the Imaging Network of the German Center for Neurodegeneration. For quality assurance and assessment, several steps were taken. The German Center for Neurodegeneration imaging network qualified each MRI site with a traveling head measurement prior to the start of the study and then provided every site with detailed standard operating procedures for the implementation of each protocol. All radiographers who operated MRIs in the study underwent centralized training to implement the standard operating procedures (ie, participants' positioning in the MRI scanner, sequence preparation steps, image angulation, participant instruction, and testing). A small MRI phantom built and designed by the American College of Radiology was used to monitor the performance of the MRI systems on a weekly basis. In addition, all scans had to pass a semiautomated check for conformity and scan quality during the data collection.

We included a bias field correction using the Advanced Normalization Tools software (http://stnava.github.io/ANTs). Spatially normalized T1 data were compared voxel-wise by using a conventional voxel-based morphometry (VBM) tool[28] for whole-brain analysis and the spatially unbiased infratentorial template (SUIT) with the corresponding toolbox for the cerebellar-focused analysis.[29] Both tools are included in the MATLAB-based statistical parametric mapping toolbox (MathWorks, Natick, Massachusetts, USA, https://www.fil.ion.ucl.ac.uk/spm/software/spm12). For SUIT-based analysis, all automatically generated cerebellar masks were visually inspected and, where necessary, manually corrected using FSLView as a part of the University of Oxford Centre for Functional MRI of the Brain, UK, (FMRIB) Software Library.[30] For spatial normalization in both pipelines, we used the Diffeomorphic Anatomical Registration using the exponentiated lie algebra algorithm with default settings including the multiplication by the determinate of the Jacobian matrix of deformation fields (modulation) to preserve local tissue volume during normalization.[29,31] For whole-brain VBM, gray and white matter probability segments were smoothed with a 8-mm Gaussian smoothing kernel (full-width at half-maximum (FWHM) = 8 mm), whereas for the SUIT pipeline cerebellar gray and white matter segments were smoothed using a 4-mm Gaussian kernel (FWHM = 4 mm).

Diffusion data were analyzed by using tract-based spatial statistics (TBSS)[32] for whole-brain analysis, as included in the FMRIB Software Library.[30] For tract-based regional analysis, we performed automated fiber-tract quantification (https://github.com/yeatmanlab/AFQ).[33] Diffusion data were preprocessed. First, all 30 within-subject diffusion-weighted images were aligned to the b0 scan. Affine transformations were calculated using the Advanced Normalization Tools software. Second, two preprocessing pipelines were used in this study: for the TBSS analysis, preprocessing included eddy current correction and tensor fitting as provided within the FMRIB's diffusion toolbox (https://fsl.fmrib.ox.ac.uk/fsl/fslwiki/FDT). For regional analysis, preprocessing also included eddy current correction and tensor-fitting steps, as included in the Vistasoft mrDiffusion software distribution (https://github.com/vistalab/vistasoft/, Stanford University, CA, USA). For TBSS analysis, we computed a study-wise space using the Advanced Normalization Tools software routines. Subsequently, all coregistered fractional anisotropy (FA) datasets were skeletonized. Skeletonized FA data were used for the statistical analysis. For FA analysis in specific fiber tracts, we used the fiber-tract quantification method (details about the tracking procedure for automated fiber-tract quantification are described in Yeatman and colleagues[33]). Their method can be briefly summarized as follows: first, the fanning out ends of tracts are cut; next, the medial, white matter associated part of each tract is subdivided into 100 equidistant nodes along the tract trajectory; and finally, for every node, a weighted mean FA value is calculated, resulting in a tract diffusion profile. The variation of FA along the tracts is the result of anatomical and geometric characteristics of each particular tract, for example, curvature, branching, or crossing fibers.[33] The tracking was performed in subject space. Therefore, spatial normalization was not required. Measurements were carried out following the automated fiber-tract quantification toolbox[33] in the forceps major and minor of the corpus callosum, cingulum, uncinate and arcuate fasciculus, and inferior and

superior longitudinal fasciculi as well as the inferior fronto-occipital fasciculus, the thalamic radiation, and the corticospinal tract. In addition to the FA, we delineated the values of radial diffusivity (RD) and axial diffusivity (AD) along the aforementioned fiber tracts.

Statistical Analysis

To examine the structural difference between groups, we set up a general linear model including scanner, age, and gender as well as total intracranial volume as nuisance covariates to account for their effects on brain structure. As the groups differed with respect to site at which the scan was performed, year of scan, and, for the diffusion tensor imaging (DTI) analysis, angulation of the scan, we also included these parameters as covariates of no interest. In addition, we performed analyses within the patient group including disease duration and SARA as additional covariates in the respective statistical models testing for group differences and performed analyses testing the correlation of disease duration and SARA with the gray and white matter alteration (VBM) and alterations in FA, RD, and AD (TBSS, tract-based regional analyses). INAS was not included because nonataxia signs characterized the MSA-C group leading to a (nonorthogonal) alignment of the parameters group (MSA-C vs. SAOA) and INAS. For the whole-brain and cerebellar voxel-wise analyses, we applied 2-sample *t* tests for each group comparison and gray and white matter segments were compared separately. We only included voxels in each analysis with tissue class probabilities greater than 20%. Statistical cut-offs included family-wise error correction (FWE) for multiple comparisons. We considered voxels with a P_{FWE} <0.01 as significant. Only clusters with an extend threshold of 10 were accepted. Effect sizes were calculated using Cohen's d. For the TBSS analysis, the threshold-free cluster enhancement method was applied with default settings. The statistical cut-off was set to P_{FWE} <0.01.

For tract-based regional FA, AD, and RD analysis, we carried out an analysis of covariance with the same covariates that were included in the whole-brain analysis models for each of the 100 nodes along each tract. Bonferroni correction was applied to correct for multiple comparisons. Group differences with a Bonferroni-corrected *P* value of $P < 0.001$ were considered significant.

For each analysis, we only accepted results that have been corrected for multiple comparisons at the most stringent significance level.

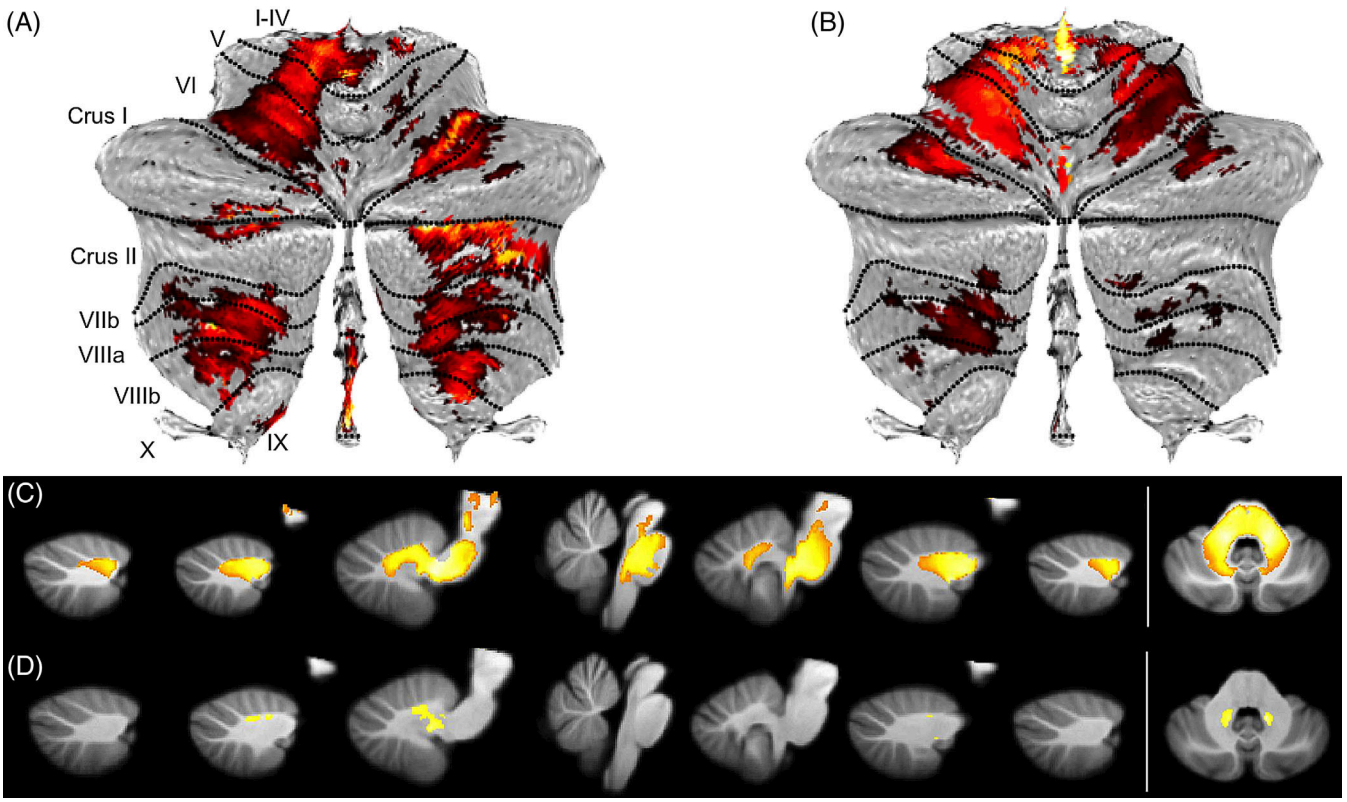

FIG. 1. Cerebellar focused voxel-based morphometry analysis in multiple system atrophy with predominant cerebellar ataxia and sporadic adult-onset ataxia compared with healthy controls ($P_{FWE} < 0.01$). (**A**) Gray matter atrophy projected onto a cerebellar flatmap in multiple system atrophy with predominant cerebellar ataxia. (**B**) Gray matter atrophy in sporadic adult-onset ataxia. (**C**) White matter atrophy projected on 7 sagittal and 1 axial slice in multiple system atrophy with predominant cerebellar ataxia. (**D**) White matter atrophy in sporadic adult-onset ataxia. [Color figure can be viewed at wileyonlinelibrary.com]

Results

Demographic and clinical data of the study population are given in Table 1 and Supporting Information Table 3. MSA-C patients, SAOA patients, and healthy controls did not differ with respect to age and sex distribution. When compared with the SAOA patients, disease duration in the MSA-C patients was shorter ($P < 0.01$), and the SARA and INAS count were higher ($P < 0.01$). Urinary dysfunction and orthostatic dysregulation ($P < 0.01$) as well as hyperreflexia ($P < 0.05$) and rigidity ($P < 0.01$) were significantly more frequent in the MSA-C patients when compared with the SAOA patients.

Whole-brain VBM did not reveal differences in gray or white matter volume between the MSA-C and SAOA patients, but the cerebellar gray and white matter of both patient groups were reduced when compared with healthy controls (Supporting Information Fig. 1). Furthermore, brainstem white matter in the MSA-C patients was reduced when compared with the healthy controls (Supporting Information Fig. 1).

The cerebellar VBM analysis using the SUIT toolbox returned gray matter volume reductions of both patient groups relative to healthy controls. Gray matter volume loss in patients was primarily found in the cerebellar areas subserving sensorimotor functions (Fig. 1).[34] The distribution of cerebellar gray matter volume loss was almost comparable in the SAOA and MSA-C patients, each in comparison with healthy controls. There was no significant difference between the SAOA and MSA-C patients. Cerebellar white matter was likewise reduced in both patient groups when compared with healthy controls. The MSA-C patients showed pronounced white matter loss in the cerebellum, the middle cerebellar peduncles, and the brainstem in comparison with healthy controls, whereas the SAOA patients in comparison with healthy controls only showed white matter loss in the cerebellar regions and middle cerebellar peduncles, but not the brainstem. The difference between the MSA-C and SAOA patients did not reach statistical significance.

When including disease duration and SARA as additional covariates in the statistical models, we did not find any significant difference between the MSA-C and SAOA patients, neither in the whole brain nor in the cerebellar VBM.

The effect sizes of the peak voxel in the whole-brain and cerebellar-focused gray and white matter VBM, for the comparison of MSA-C patients as well as for the comparison of SAOA patients with healthy controls were >1 (for details, see Supporting Information Table 5).

TBSS revealed reduced FA in the MSA-C patients both in comparison with the SAOA patients and healthy controls. Relative to healthy controls, the FA in the MSA-C patients was reduced in the pontine regions, the middle cerebellar peduncles, and the central portion of cerebellar white matter. Thus, major parts of the

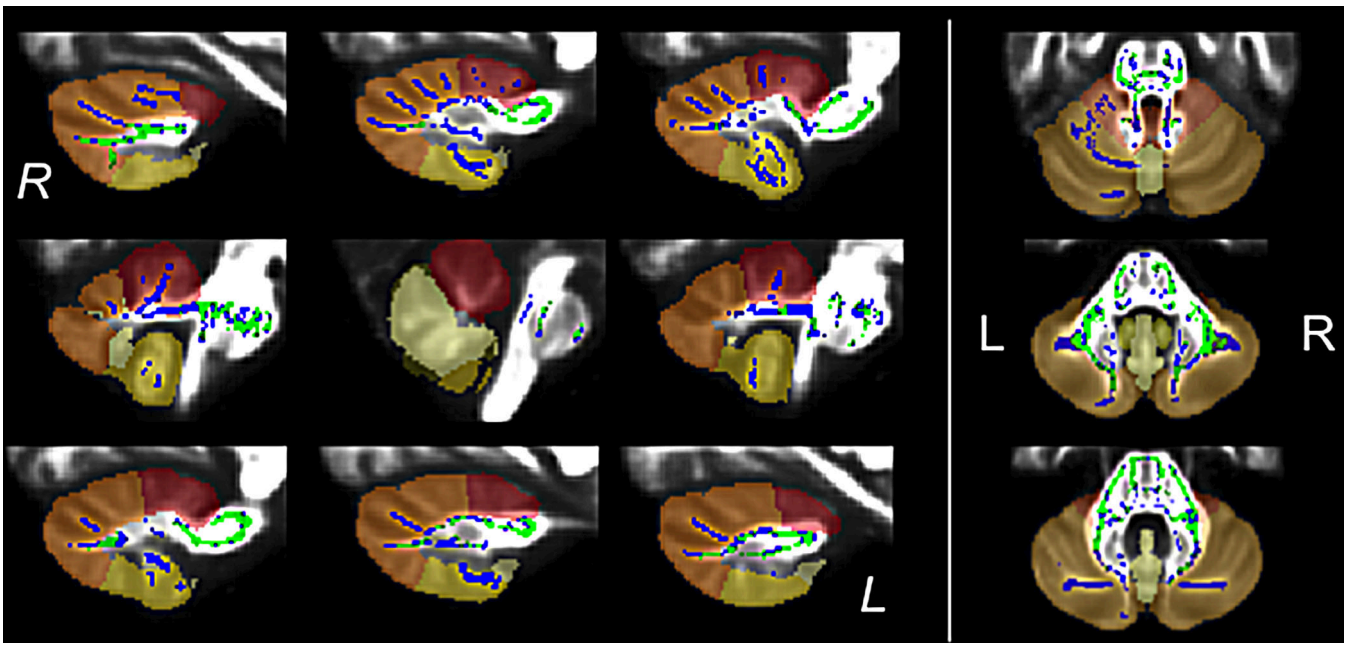

FIG. 2. Tract-based spatial statistics of fractional anisotropy in multiple system atrophy with predominant cerebellar ataxia compared with sporadic adult-onset ataxia and healthy controls. Reductions in multiple system atrophy with predominant cerebellar ataxia compared to sporadic adult-onset ataxia are shown in green, and reductions compared with healthy controls in blue ($P_{FWE} < 0.01$). Data are presented on 9 sagittal and 3 axial slices. The cerebellar subregions are colored for anatomical reference: anterior cerebellum in red, superior posterior cerebellum in orange, the inferior posterior cerebellum in yellow, and the vermis in bright yellow. [Color figure can be viewed at wileyonlinelibrary.com]

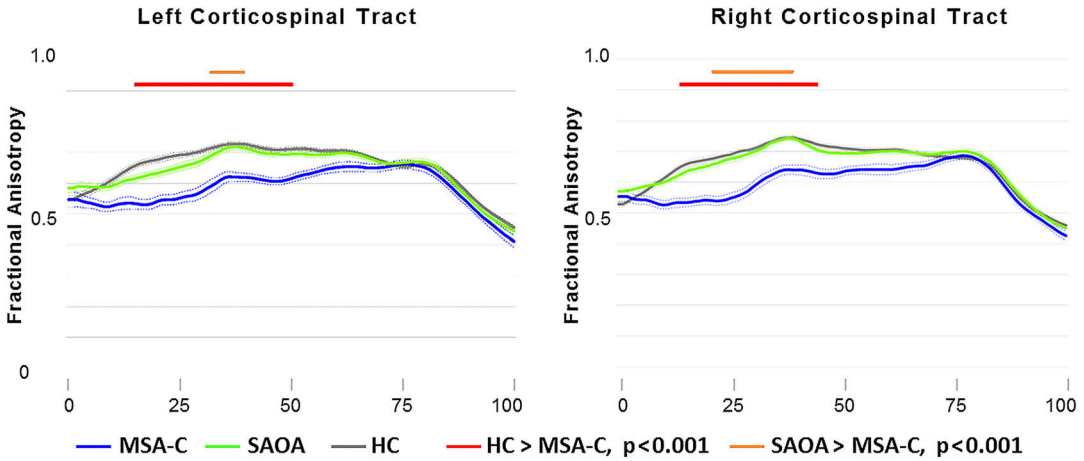

FIG. 3. Tractography-based regional analysis of fractional anisotropy along the corticospinal tract. Mean fractional anisotropy is given for multiple system atrophy with predominant cerebellar ataxia (MSA-C; blue), sporadic adult-onset ataxia (SAOA; green), and healthy controls (HC, gray). Sections of the corticospinal tract with significantly reduced fractional anisotropy in MSA-C compared with healthy controls are marked with a red line, and those with reduced fractional anisotropy compared with SAOA with an orange line ($P < 0.001$, Bonferroni). [Color figure can be viewed at wileyonlinelibrary.com]

anterior and posterior cerebellum (including white matter branching into the lobules I–IV bilaterally, V and VI right-sided, crus I, crus II, and lobule VIIb, VIIIb, and X bilaterally) were affected (Fig. 2). The comparison of MSA-C and SAOA patients revealed a similar, but less extended, pattern of FA reduction in the MSA-C patients (Fig. 2), involving the superior posterior part of the cerebellum including white matter branching into crus II bilaterally and lobule VIIb on the right side. The comparison of the SAOA patients with healthy controls did not reveal FA reduction in SAOA patients. However, there was a patchy pattern of increased FA in the SAOA patients around the left thalamus (Supporting Information Fig. 2). When adding disease duration or SARA sum score as an additional covariate in the statistical model, the distribution of decreased FA in the MSA-C patients in comparison with healthy controls was slightly less expanded, but the overall pattern remained unchanged (Supporting Information Fig. 2b and 2c).

We delineated the FA along the medial white matter–associated portion of the forceps major and minor of the corpus callosum and along the cingulum, uncinate, arcuate, inferior, and superior longitudinal and inferior fronto-occipital fasciculi, the thalamic radiation, and the corticospinal tracts across both hemispheres. Of note, the automated tracking method failed in only 29 times of 1764 total tracking attempts. The variation of the FA along the trajectories was consistent with previous reported tract characteristics for all tracts.[33] In the MSA-C group, the FA was reduced along the corticospinal tracts bilaterally both in comparison with healthy controls and SAOA patients (Fig. 3). However, the distribution of abnormalities was more widespread for the comparison with healthy controls than with the SAOA patients. In the right arcuate tract of the SAOA patients, the FA was reduced over a short distance representing less than 10% of the tract length (Supporting Information Fig. 3). No other significant group differences were detected.

In the delineation of AD and RD along the aforementioned white matter tracts, we did not find consistent patterns of alterations. There was a trend of increased RD in patients in comparison with healthy controls, but significant group differences were only observed in short distances representing less than 10% of the respective tracts. In detail, RD was increased in the MSA-C patients in both corticospinal tracts and the superior longitudinal fasciculus and the forceps minor of the corpus callosum in the SAOA patients, each in the comparison of the respective patient group with the group of healthy controls. AD was increased in both corticospinal tracts and the left inferior longitudinal fasciculus in the MSA-C patients and in the SAOA patients in the forceps minor of the corpus callosum and the left inferior fronto-occipital fasciculus. No significant differences between both patient groups were observed (Supporting Information Fig. 3).

There was no significant difference in the FA values along the corticospinal tract between MSA-C patients with or without pyramidal signs (for details, see Supporting Information Fig. 3d).

Discussion

This comparative MRI study provides a detailed analysis of brain volume changes and white matter microstructural alterations in MSA-C and SAOA. The gray matter volume loss detected by VBM had a similar

extent in both patient groups, which primarily involved the sensorimotor regions of the cerebellar cortex. In MSA-C, there was additional white matter volume loss in the cerebellum and brainstem. In SAOA, however, cerebellar white matter volume was only slightly reduced, and the brainstem was relatively preserved. DTI revealed widespread microstructural alterations of white matter in the MSA-C patients affecting the cerebellum, brainstem, and corticospinal tracts that were mostly absent in the SAOA patients.

A strength of our study is the multimodal approach that thoroughly assessed the structural integrity of brain gray and white matter tissue with different state-of-the-art MRI methods. This approach provides a more comprehensive view of brain morphology than that of previous studies focusing on either structural volume or DTI changes alone.[7,13,15,17,19,23,35-40]

Previous volumetric and VBM studies in MSA-C have consistently shown cerebellar and brainstem volume loss.[13,15,17,19,20,35-37,40] In SAOA, volume loss has been reported as being most prominent in the cerebellum, although some studies also detected involvement of the cerebellar peduncles and brainstem. A volumetric MRI study directly comparing MSA-C and SAOA found that the pattern of cerebellar atrophy was similar in both groups, but the brainstem volume was smaller in MSA-C than in SAOA.[15] The results of our study are consistent with these findings. In addition, they indicate that the loss of brainstem volume in MSA-C is mainly the result of the loss of white matter. We also found that in both patient groups, gray matter atrophy was most prominent in the sensorimotor regions of the cerebellum. Some of the previous volumetric and VBM studies reported gray matter loss in the basal ganglia and cortical regions in MSA-C patients.[13,19] We could not replicate those findings. This might be because of our small sample size and the very stringent significance level we applied to reduce the likelihood of false positive results.

Previous DTI studies in MSA-C reported abnormal diffusion parameters in the brainstem, most notably the pons, middle cerebellar peduncles, and cerebellar white matter.[22] In addition, supratentorial white matter, notably the corticospinal tract, internal capsule, corpus callosum, corona radiata, and cingulum were also affected.[16,17,21-23,41] In an early DTI study of 3 SAOA patients, an increase of the apparent diffusion coefficient, interpreted as a loss of white matter integrity, was found in the cerebellum and brainstem.[42] Another study directly comparing MSA-C and SAOA found markedly reduced FA values in afferent cerebellar tracts in MSA-C that allowed a fairly good discrimination from SAOA.[18] The results of our study confirm the presence of widespread white matter abnormalities in MSA-C, as indicated by reduced FA, affecting not only brainstem and cerebellar fiber tracts but also the corticospinal tracts. In contrast, there were only negligible FA abnormalities in SAOA. FA is a widely used diffusion parameter to describe microstructural alterations of white matter in the brain. The additional analysis of AD and RD did not show any consistent and extended alterations that one could consider as relevant, although RD showed a strong trend toward an increase in MSA-C patients (for details, see Supporting Information Fig. 3c).

The principal finding of this study is the prominent white matter involvement in MSA-C that distinguished MSA-C from SAOA. This corresponds well to the results of a postmortem study showing that cerebellar white matter degeneration in MSA was more pronounced than that of the cerebellar cortex.[43] Imaging and autopsy evidence of major white matter pathology in MSA is consistent with characterization of this disease as a primary oligodendrogliopathy.[44]

When compared with SAOA, MSA-C has a more severe phenotype and faster disease progression.[11] This is also reflected by the characteristics of the patient groups of this study. SARA and INAS scores of the MSA-C patients were higher than those of the SAOA patients, although the disease duration of the MSA patients was shorter. Including ataxia severity as a covariate in the analysis did not change the results in the group comparison, and we did not find any positive or negative correlation of SARA with gray or white matter volume or FA on the high significance level corrected for multiple comparisons. Because the observed group differences between MSA-C and SAOA were not influenced by ataxia severity, they rather reflect substantial differences in the brain pathology of MSA-C patients in comparison with SAOA patients.

The MSA-C patients showed a higher prevalence of clinical pyramidal tract signs than the SAOA patients. Correspondingly, an affection of the corticospinal tracts was observed in the MSA-C patients, but not in the SAOA patients.[11,16] A direct comparison of MSA-C patients with and without pyramidal tract signs did not reveal differences. Because of the very small subgroups, this analysis should be considered with caution. Nevertheless, these results underline the significance of disease-specific white matter alterations in MSA-C that are not present in SAOA.

As part of the prospective SPORTAX natural history study, all patients underwent an extensive clinical characterization including careful consideration of inclusion/exclusion criteria and diagnostic categories.[11] Nevertheless, this study, as all others in the field of sporadic degenerative ataxia, has to contend with the problem that some patients initially diagnosed as SAOA may develop severe autonomic failure at later time points requiring a change of the clinical diagnosis to MSA-C.[6,11] As the disease duration was considerably longer in the SAOA when compared with the MSA-C group, we are confident that the number of such future

"converters" in the SAOA group was low; however, within this ongoing prospective study the postmortem diagnostic confirmation was not available. Additional limitations of our study are the relatively small number of study subjects, lack of follow-up, and the uneven distribution of patients between the 2 study sites. To account for these limitations and reduce the likelihood of false positive results, we included additional covariates in the statistical analysis and reported only results with highly stringent statistical thresholds. By doing so, we may have underestimated effects and group differences.

In the multimodal imaging of our deeply phenotyped cohort, we did not find any differences in gray and white matter volumes between the MSA-C and SAOA patients, but a clear contrast of microstructural white matter alterations between the MSA-C and SAOA patients. The MSA-C patients showed alteration in the microstructure of the brainstem and cerebellar white matter as well as the corticospinal tract. Our results suggest that DTI abnormalities may aid the early diagnostic distinction between these 2 conditions, which remains a clinical challenge.[45] To this end, longitudinal studies of larger cohorts are required. In this respect, longitudinal DTI studies of SAOA patients that convert to MSA-C would be particularly informative. ■

Acknowledgment: We thank all patients and volunteers who participated in this study. We thank Frank Jessen, Department of Psychiatry, University of Cologne, for the contribution of control data from the DELCODE (German Center for Neurodegenerative Diseases (DZNE)–Longitudinal Cognitive Impairment and Dementia Study). We thank Heike Jacobi, Ina Vogt, and Marcus Grobe-Einsler for their assistance in the study execution.

References

1. Schols L, Szymanski S, Peters S, et al. Genetic background of apparently idiopathic sporadic cerebellar ataxia. Hum Genet 2000;107(2):132–137.
2. Moseley ML, Benzow KA, Schut LJ, et al. Incidence of dominant spinocerebellar and Friedreich triplet repeats among 361 ataxia families. Neurology 1998;51(6):1666–1671.
3. Abele M, Burk K, Schols L, et al. The aetiology of sporadic adult-onset ataxia. Brain 2002;125(5):961–968.
4. Wakabayashi K, Hayashi S, Kakita A, et al. Accumulation of alpha-synuclein/NACP is a cytopathological feature common to Lewy body disease and multiple system atrophy. Acta Neuropathol 1998;96(5):445–452.
5. Trojanowski JQ, Revesz T, Neuropathology Working Group on MSA. Proposed neuropathological criteria for the post mortem diagnosis of multiple system atrophy. Neuropathol Appl Neurobiol 2007;33(6):615–620.
6. Gilman S, Wenning GK, Low PA, et al. Second consensus statement on the diagnosis of multiple system atrophy. Neurology 2008;71(9):670–676.
7. Abele M, Minnerop M, Urbach H, Specht K, Klockgether T. Sporadic adult onset ataxia of unknown etiology: a clinical, electrophysiological and imaging study. J Neurol 2007;254(10):1384–1389.
8. Harding AE. "Idiopathic" late onset cerebellar ataxia. A clinical and genetic study of 36 cases. J Neurol Sci 1981;51(2):259–271.
9. Tsuchiya K, Ozawa E, Saito F, Irie H, Mizutani T. Neuropathology of late cortical cerebellar atrophy in Japan: distribution of cerebellar change on an autopsy case and review of Japanese cases. Eur Neurol 1994;34(5):253–262.
10. Ota S, Tsuchiya K, Anno M, Niizato K, Akiyama H. Distribution of cerebello-olivary degeneration in idiopathic late cortical cerebellar atrophy: clinicopathological study of four autopsy cases. Neuropathology 2008;28(1):43–50.
11. Giordano I, Harmuth F, Jacobi H, et al. Clinical and genetic characteristics of sporadic adult-onset degenerative ataxia. Neurology 2017;89(10):1043–1049.
12. Klockgether T. Sporadic adult-onset ataxia. Handb Clin Neurol 2018;155:217–225.
13. Brenneis C, Boesch SM, Egger KE, et al. Cortical atrophy in the cerebellar variant of multiple system atrophy: a voxel-based morphometry study. Mov Disord 2006;21(2):159–165.
14. Burk K, Buhring U, Schulz JB, Zuhlke C, Hellenbroich Y, Dichgans J. Clinical and magnetic resonance imaging characteristics of sporadic cerebellar ataxia. Arch Neurol 2005;62(6):981–985.
15. Burk K, Globas C, Wahl T, et al. MRI-based volumetric differentiation of sporadic cerebellar ataxia. Brain 2004;127(Pt 1):175–181.
16. da Rocha AJ, Maia AC Jr, da Silva CJ, et al. Pyramidal tract degeneration in multiple system atrophy: the relevance of magnetization transfer imaging. Mov Disord 2007;22(2):238–244.
17. Dash SK, Stezin A, Takalkar T, et al. Abnormalities of white and grey matter in early multiple system atrophy: comparison of parkinsonian and cerebellar variants. Eur Radiol 2019;29(2):716–724.
18. Fukui Y, Hishikawa N, Sato K, et al. Characteristic diffusion tensor tractography in multiple system atrophy with predominant cerebellar ataxia and cortical cerebellar atrophy. J Neurol 2016;263(1):61–67.
19. Minnerop M, Specht K, Ruhlmann J, et al. Voxel-based morphometry and voxel-based relaxometry in multiple system atrophy-a comparison between clinical subtypes and correlations with clinical parameters. Neuroimage 2007;36(4):1086–1095.
20. Yang H, Wang N, Luo X, et al. Cerebellar atrophy and its contribution to motor and cognitive performance in multiple system atrophy. Neuroimage Clin 2019;23:101891.
21. Zanigni S, Evangelisti S, Testa C, et al. White matter and cortical changes in atypical parkinsonisms: a multimodal quantitative MR study. Parkinsonism Relat Disord 2017;39:44–51.
22. Heim B, Krismer F, Seppi K. Structural imaging in atypical parkinsonism. Int Rev Neurobiol 2018;142:67–148.
23. Wang PS, Wu HM, Lin CP, Soong BW. Use of diffusion tensor imaging to identify similarities and differences between cerebellar and parkinsonism forms of multiple system atrophy. Neuroradiology 2011;53(7):471–481.
24. Wang PS, Yeh CL, Lu CF, Wu HM, Soong BW, Wu YT. The involvement of supratentorial white matter in multiple system atrophy: a diffusion tensor imaging tractography study. Acta Neurol Belg 2017;117(1):213–220.
25. Wenning GK, Tison F, Seppi K, et al. Development and validation of the Unified Multiple System Atrophy Rating Scale (UMSARS). Mov Disord 2004;19(12):1391–1402.
26. Schmitz-Hubsch T, du Montcel ST, Baliko L, et al. Scale for the assessment and rating of ataxia: development of a new clinical scale. Neurology 2006;66(11):1717–1720.
27. Jacobi H, Rakowicz M, Rola R, et al. Inventory of Non-Ataxia Signs (INAS): validation of a new clinical assessment instrument. Cerebellum 2013;12(3):418–428.
28. Ashburner J, Friston KJ. Voxel-based morphometry—the methods. Neuroimage 2000;11(6 Pt 1):805–821.
29. Diedrichsen J, Balsters JH, Flavell J, Cussans E, Ramnani N. A probabilistic MR atlas of the human cerebellum. Neuroimage 2009;46(1):39–46.
30. Smith SM, Jenkinson M, Woolrich MW, et al. Advances in functional and structural MR image analysis and implementation as FSL. Neuroimage 2004;23(suppl 1):S208–S219.

31. Ashburner J. A fast diffeomorphic image registration algorithm. Neuroimage 2007;38(1):95–113.

32. Smith SM, Jenkinson M, Johansen-Berg H, et al. Tract-based spatial statistics: voxelwise analysis of multi-subject diffusion data. Neuroimage 2006;31(4):1487–1505.

33. Yeatman JD, Dougherty RF, Myall NJ, Wandell BA, Feldman HM. Tract profiles of white matter properties: automating fiber-tract quantification. PLoS One 2012;7(11):e49790.

34. Diedrichsen J, Zotow E. Surface-based display of volume-averaged cerebellar imaging data. PLoS One 2015;10(7):e0133402.

35. Krismer F, Wenning GK. Multiple system atrophy: insights into a rare and debilitating movement disorder. Nat Rev Neurol 2017; 13(4):232–243.

36. Hauser TK, Luft A, Skalej M, et al. Visualization and quantification of disease progression in multiple system atrophy. Mov Disord 2006;21(10):1674–1681.

37. Specht K, Minnerop M, Muller-Hubenthal J, Klockgether T. Voxel-based analysis of multiple-system atrophy of cerebellar type: complementary results by combining voxel-based morphometry and voxel-based relaxometry. Neuroimage 2005;25(1):287–293.

38. Villanueva-Haba V, Garces-Sanchez M, Bataller L, Palau F, Vilchez J. Neuroimaging study with morphometric analysis of hereditary and idiopathic ataxia. Neurologia 2001;16(3):105–111.

39. Wullner U, Klockgether T, Petersen D, Naegele T, Dichgans J. Magnetic resonance imaging in hereditary and idiopathic ataxia. Neurology 1993;43(2):318–325.

40. Specht K, Minnerop M, Abele M, Reul J, Wullner U, Klockgether T. In vivo voxel-based morphometry in multiple system atrophy of the cerebellar type. Arch Neurol 2003;60(10):1431–1435.

41. Blain CR, Barker GJ, Jarosz JM, et al. Measuring brain stem and cerebellar damage in parkinsonian syndromes using diffusion tensor MRI. Neurology 2006;67(12):2199–2205.

42. Della Nave R, Foresti S, Tessa C, et al. ADC mapping of neurodegeneration in the brainstem and cerebellum of patients with progressive ataxias. Neuroimage 2004;22(2):698–705.

43. Matsusue E, Fujii S, Kanasaki Y, Kaminou T, Ohama E, Ogawa T. Cerebellar lesions in multiple system atrophy: postmortem MR imaging-pathologic correlations. Am J Neuroradiol 2009;30(9):1725–1730.

44. Wenning GK, Stefanova N, Jellinger KA, Poewe W, Schlossmacher MG. Multiple system atrophy: a primary oligodendrogliopathy. Ann Neurol 2008;64(3):239–246.

45. Kim HJ, Jeon B, Fung VSC. Role of magnetic resonance imaging in the diagnosis of multiple system atrophy. Mov Disord Clin Pract 2017;4(1):12–20.

Supporting Data

Additional Supporting Information may be found in the online version of this article at the publisher's web-site.